

Improving Efficiency and Response of Photovoltaic Power Generation with DC/DC Buck Converter

Le Tien Phong

Electrical Faculty

Thai Nguyen University of Technology
Thai Nguyen, Viet Nam

Ngo Duc Minh

Electrical Faculty

Thai Nguyen University of Technology
Thai Nguyen, Viet Nam

Nguyen Van Lien

Electrical Institute

Ha Noi University of Technology and Science
Ha Noi, Viet Nam

Abstract—This paper presents two new methods using the same structure to control photovoltaic power generation. They are combined the iterative and bisectional technique with average voltage control called IB-AVC method and sliding mode control called IB-SMC method to capture and maintain the operation point of PVg at maximum power point with a DC/DC buck converter. The iterative and bisectional technique in maximum power point tracker is used to identify parameters at maximum power point that provides the destination for controllers basing on the analysis of moving statement of operation points, a system of equations to describe the change of its parameters and informations about intensity of solar irradiance and temperature on this generation. Simulation results show that IB-AVC and IB-SMC methods can bring the highest efficiency (approximately 100%). They also represents static and dynamic responses better than traditional control methods and when it operating this generation under variable weather conditions.

Index Terms—Average voltage control, iterative and bisectional technique, maximum power point, maximum power point tracker, photovoltaic power generation, sliding mode control.

I. INTRODUCTION

Basically, all efforts to increase efficiency of photovoltaic power generation (PVg) up to more some percentages by manufacturing meet difficulties because of limiting material and production engineering. The special characteristic of PVg is that always exists an operation state corresponding with the available maximum power. For a fixed power implement, the amount of power generating from PVg depends on value of intensity of solar irradiance (G), temperature on PVg (T) and electrical load (characterized by impedance of load g_{load}). So, maximum power point (MPP) can be reached by combining control techniques with a maximum power point tracker (MPPT) to drive voltage, current or power at input power converters to desired values.

Average voltage control (AVC), sliding mode control (SMC) and AI (Artificial Intelligence) are often used as control techniques in systems exploiting PVg. For AVC technique, PVg is considered as a voltage source and controlled by double feedback control loops (current and voltage loops) to place output voltage of PVg at desired voltage [1], [2], [3]. For

SMC technique, destinations at any condition for PVg are often voltage, power, impedance and they are also sliding surfaces for controllers [4-11]. Above techniques only help controllers change load for PVg, so efficiency and responses in the process of exploiting PVg depend on characteristics of MPPT. Another control technique, only using AI (Artificial Intelligence), a pyranometer (PYR) and a temperature sensor (TempS), needs much time to collect data, recalculates parameters of controller corresponding to any type of PVg and require a large memory to save data acquisition [12]. Because of above reason, AVC and SMC are more popular than AI to control PVg.

Simultaneously, traditional techniques for MPPT are classified into online and offline groups. Online techniques actively change control pulse before having considerations about MPP whereas offline techniques calculate parameters at MPP in internal controllers before creating control pulse.

For online techniques, SC (Short-Circuit Current) or OV (Open-Circuit Voltage) technique causes short-circuit or open-circuit to measure value of short-circuit current (I_{sc}) or open-circuit voltage (V_{oc}) [13], [14]; P&O (Perturb and Observe) and INC (Incremental Conductance) try to reach to MPP by changing Δd (pulse control step) continuously [13], [15], [16], [17]. Another approach to find MPP is that combines P&O with AI to reduce Δd when the operation point is near MPP [18]. Because of being a weak generation when operating at far STC (Standard Test Condition), controllers using above techniques always make perturbation, power loss, and easily to have wrong evaluations about MPP.

For offline techniques, CV (Constant Voltage) is the simplest technique due to using only voltage sensor [13], Temp (temperature) technique only uses a temperature sensor (TempS) [19]. They also provide unexactly about MPP when real weather operation is far STC. Ref. [20] proposed another technique, called OG (Optimal Gradient), to find MPP but it has to use the simple model for PVg to reduce calculation quantity for the controller and TempS, pyranometer (PYR). Common idea for offline technique is to set a fixed value for controllers and maintain the operation point at that value to reduce perturbation in control circuit. Basing on above idea, IB

technique was introduced as an offline technique to identify exact parameters at MPP for any types of PVg and any weather conditions in own controller using the information about G, T and parameters of PVg provided by manufacturers [21]. Nowadays, PYR and TempS are more sensitive, more suitable, cheaper and more popular, so IB technique is easier to apply in system exploiting PVg.

To improve efficiency and response of PVg, it needs to be driven to new MPP immediately when having any change of (G, T) and maintain at MPP when not having any change of (G, T). To do this idea, two new methods are proposed in this paper to control PVg, called IB-AVC and IB-SMC. Although using the same structure, IB-AVC method combines the IB technique with AVC technique whereas IB-SMC method combines the IB technique with SMC technique. Due to above purposes, the rest of the paper is organized as follows: Section II is for the system structure and modelling. Section III introduces IB technique to identify MPP. Section IV designs controllers. Section V provides an illustrative example to show the effectiveness of proposed methods and Section IV presents some conclusions where the significant points and remarks of the paper are summarized.

II. SYSTEM STRUCTURE AND MODELLING

A. System structure

The system structure is described in Fig. 1.

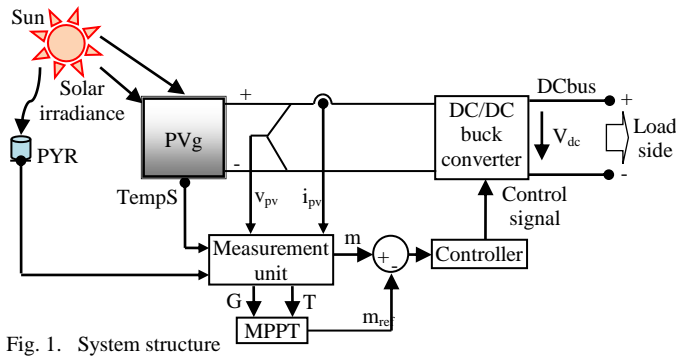


Fig. 1. System structure

where:

Measurement unit collects all information about G from PYR, temperature on PVg from TempS, instantaneous current and voltage of PVg from sensors placed at output terminals.

MPPT uses the IB technique to calculate desired values (voltage v_{mpp} , current i_{mpp} or power P_{mpp} at MPP) at instantaneous time.

The controller uses informations about m from measurement unit and m_{ref} from MPPT to evaluate and decide pulse control. For AVC controller, m_{ref} is V_{mpp} . For SMC controller, sliding surface is chosen because power at MPP is the destination that needs to reach at any time, so m_{ref} is P_{mpp} .

The DC/DC buck converter is a non-isolated converter and its output voltage is smaller than its input voltage. To operate PVg at MPP, input voltage and current of this converter is regulated corresponding with them at MPP. Moreover, to operate PVg at MPP, load side at DCbus needs to be linked to an energy storage or a DC/AC converter that is connected to

the electric grid to have a balance power between input and output for DC/DC converter. Because of this reason, voltage at DCbus is held at a fixed value by load side.

B. Modelling PVg

PVg is described as the equivalent circuit in Fig. 2 [13], [15], [17].

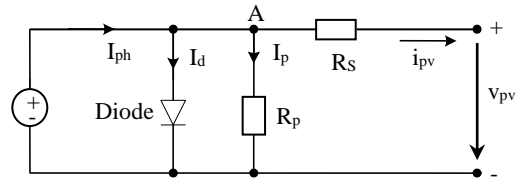


Fig. 2. Equivalent circuit of PVg

Write Kirchhoff law equation at node A:

$$i_{pv} = I_{ph} - I_0 \left\{ \exp \left(\frac{v_{pv} + i_{pv} R_s}{n V_t} \right) - 1 \right\} - \frac{v_{pv} + i_{pv} R_s}{R_p} \quad (1)$$

Instantaneous power generating from PVg:

$$P_{pv} = v_{pv} i_{pv} \quad (2)$$

where: R_s is series resistor; R_p is parallel resistor; I_0 is reserve saturation current; I_{ph} is photo-generated current; I_0 is saturation current; V_t is thermal voltage of PVg; n is diode ideality factor.

Representing equation (1) and (2), we have $v_{pv}-i_{pv}$, $v_{pv}-P_{pv}$ curves corresponding with each value of couple (G, T). Each curve always exists a peak point called MPP and it divides two curves into two sides as Fig. 3.

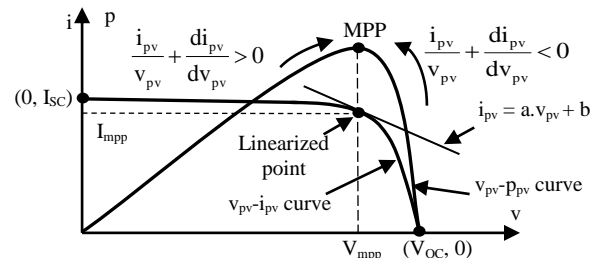


Fig. 3. $v_{pv}-i_{pv}$ and $v_{pv}-P_{pv}$ curves of PVg

In fact, datasheet for each PVg only presents some basic parameters that are: short circuit current I_{SC} , open circuit voltage V_{OC} , voltage and current at MPP (V_{mpp} , I_{mpp}) at STC, temperature coefficient of voltage C_{TV} , current C_{TI} and power C_{TP} . Unknown parameters not presenting such as I_{ph} , I_0 , V_t , R_s , R_p can be calculated by Newton-Raphson algorithm [21].

When G and T vary in real conditions, parameters of PVg are changed by (3) [21].

$$\begin{cases} I_{ph}|_{G,T} = \frac{G}{G_{stc}} \{ I_{phstc} [1 + C_{TI}(T - T_{stc})] \} \\ I_{SC}|_{G,T} = I_{SCstc} \left[\frac{G}{G_{stc}} + C_{TI}(T - T_{stc}) \right] \\ V_t|_{G,T} = V_{tstc} \frac{T}{T_{stc}} \\ V_{OC}|_{G,T} = V_{OCstc} [1 + C_{TV}(T - T_{stc})] + V_t \ln \frac{G}{G_{stc}} \\ R_p|_{G,T} = R_{pstc} \frac{G_{stc}}{G} \\ R_s|_{G,T} = R_{Sstc} \end{cases} \quad (3)$$

where, values of symbols having “stc” are defined in STC,

n is a non-linear function and can be defined by each structure of PVg.

C. DC/DC buck converter

A DC/DC buck converter can be modeled in small signal state or in switching state. Its electric circuit and equivalent circuit in above states are represented in Fig. 4 [1], [2], [3], [22].

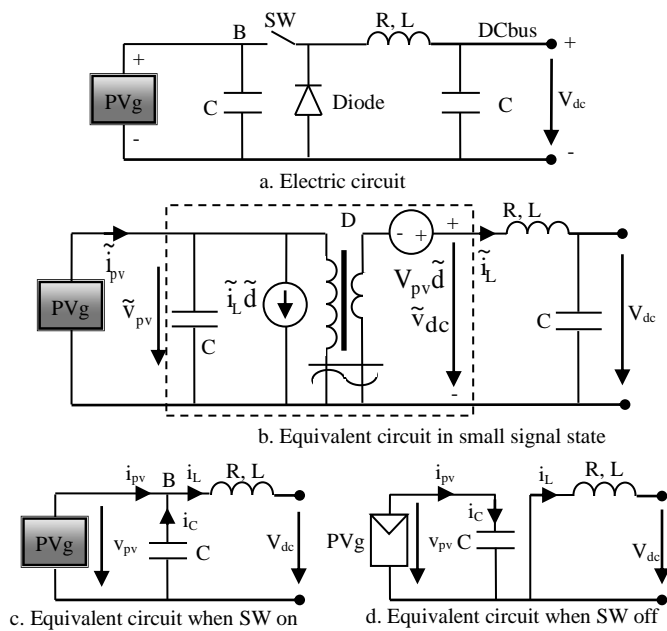


Fig. 4. Modelling a DC/DC buck converter

Where, small signal state is to obtain a small-signal transfer function and switching states is to write system of state equations. In Fig. 4, symbols having “~” are defined in small signal state or small variation of variables when pulse control changes, Vdc is output voltage of converter held at fixed value, Vpv=Vdc/D and Ipv are average values (D is voltage transformation ratio corresponding with continuous state).

III. MPPT

Because of the complexity of equation (1), Vmpp and Impp can't be identified by solving equation dpv/dvpv=0. Using detective technique for identifying couple of (vpv(i), i(i)) at ith

step and bisectional technique by observing the movement of operation points in a vpv-pvpv curve as presented in Fig. 5 (continuous arrow for present direction, dash arrow for next direction), IB technique was proposed to identify MPP. It has two stages: the first one is that moves forward normally and the second one is that bisects as represented in Fig. 6. To excute this technique at any weather condition, it need to use system of equations (3), calculate all unknown parameters of PVg and use information about G, T [21]. The algorithm using IB technique to identify MPP for PVg at any weather condition is presented in Fig. 7 [20]

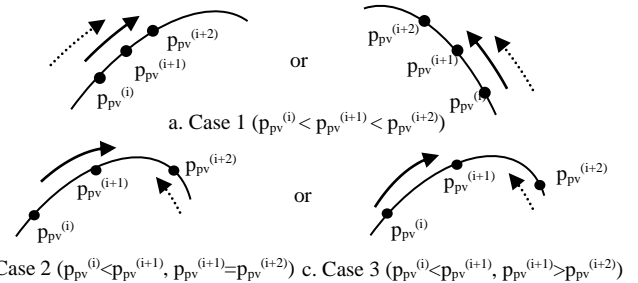


Fig. 5. Moving statement of operation points

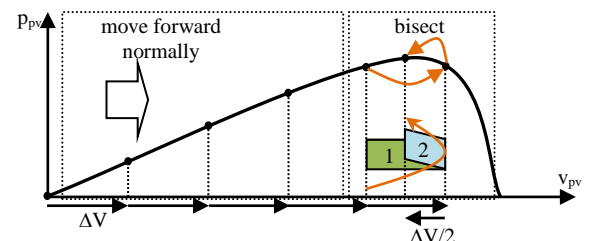


Fig. 6. The process of identifying MPP using IB technique

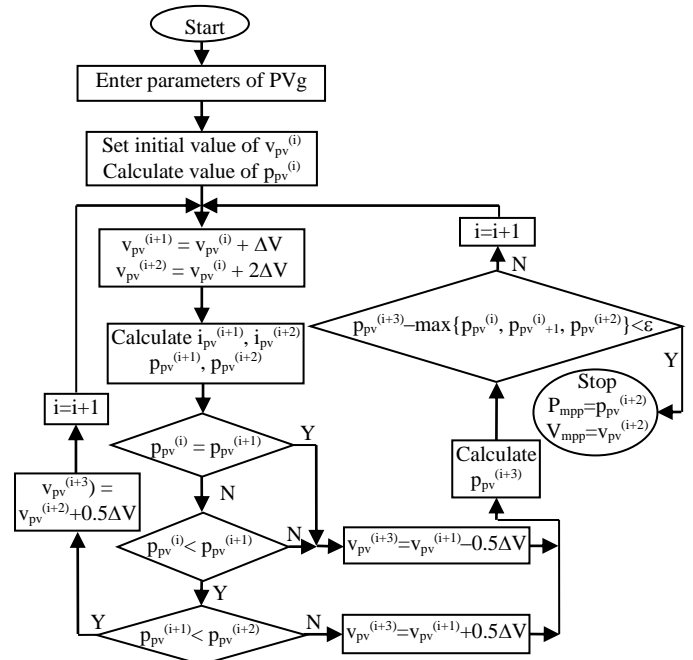


Fig. 7. Algorithm using IB technique to find MPP

where: ΔV is value of voltage step.

To ensure the convergence for this algorithm, ΔV should be chosen smaller than $(V_{OC} - V_{mpp})$. Advantages of this technique are that can apply for any type of PVg and calculate parameters at MPP in self-processor very fast whenever having any change of (G, T).

IV. DESIGN CONTROLLER

A. AVC Controller

The structure of AVC controller is presented in Fig. 8 [1], [2], [3].

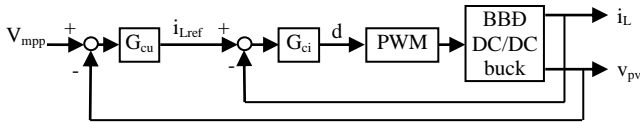


Fig. 8. Control structure of BS-AVC method

The relationships of quantities in Fig 4b are described by system of equations (4):

$$v_{pv} = V_{pv} + \tilde{v}_{pv}, i_{pv} = I_{pv} - \tilde{i}_{pv}, i_L = I_L - \tilde{i}_L, d = D - \tilde{d} \quad (4)$$

where, d is duty cycle of pulse control.

Write Kirchoff laws at DCbus side and bus B in Fig. 4b:

$$L \frac{di_L}{dt} = v_{pv}d - V_{dc} \quad (5)$$

$$i_C = i_{pv} - i_L d \quad (6)$$

Substituting equation (4) into equation (5) and using Laplace transform and conditions: $V_{dc} = DV_{pv} - RI_L$, $\tilde{v}_{pv}\tilde{d} \approx 0$, we have:

$$-(R + sL)\tilde{i}_L = -V_{pv}\tilde{d} + \tilde{v}_{pv}D \quad (7)$$

For current control loop, we have $\tilde{v}_{pv} = 0$ and current transfer function is:

$$G_{id} = \frac{\tilde{i}_L}{\tilde{d}} = \frac{V_{pv}}{R + sL} \quad (8)$$

PWM pulse transfer function for current loop:

$$G_{PWM} = \frac{1}{1 + 0.5T_s s} \quad (9)$$

where: $T_s = 1/f_s$ is time of pulse cycle.

Open-current control loop at MPP:

$$G_{ih} = G_{id}G_{PWM} = \frac{K_1}{(1 + T_1s)(1 + T_2s)} \quad (10)$$

where, $K_1 = V_{mpp}/R$, $T_1 = L/R$, $T_2 = T_s/2$.

Current controller G_{ci} :

$$G_{ci} = K_{ip} + \frac{K_{ii}}{s} \quad (11)$$

$$\text{where, } K_{ip} = \frac{T_1}{2K_1T_2}, K_{ii} = \frac{1}{2K_1T_2}$$

Linearize at stable point (MPP), we have the relation of v_{pv} and i_{pv} :

$$i_{pv} = av_{pv} + b \quad (12)$$

where,

$$\begin{cases} a = \left. \frac{di_{pv}}{dv_{pv}} \right|_{mpp} = \frac{-\frac{I_0}{V_t} \exp\left(\frac{V_{mpp} + I_{mpp}R_s}{nV_t}\right) + \frac{1}{R_p}}{1 + \frac{I_0R_s}{V_t} \exp\left(\frac{V_{mpp} + I_{mpp}R_s}{nV_t}\right) + \frac{R_s}{R_p}} < 0 \\ I_{mpp} = aV_{mpp} + b \end{cases} \quad (13)$$

Substituting equation (12) into equation (6) and using Laplace transform and conditions: $I_L D = I_{pv} = aV_{pv} + b$, $\tilde{i}_L\tilde{d} \approx 0$, $\tilde{d} = 0$, we have voltage transfer function:

$$G_{ui} = \frac{\tilde{v}_{pv}}{\tilde{i}_L} = \frac{-D/a}{1 - \frac{C}{a}s} \quad (14)$$

Open-current control loop at MPP:

$$G_{dt} = \frac{-D/a}{1 - \frac{C}{a}s} \frac{1}{1 + \frac{L}{V_{pv}K_{pi}}s} = \frac{K_2}{(1 + T_3s)(1 + T_4s)} \quad (15)$$

where, $K_2 = -D/a$, $T_3 = -C/a$, $T_4 = L/(V_{mpp}K_{pi})$

Voltage controller G_{cu} :

$$G_{cu} = K_{pu} + \frac{K_{ui}}{T_u s} \quad (16)$$

$$\text{where, } K_{up} = \frac{T_3}{2K_2T_4}, K_{ui} = \frac{1}{2K_2T_4}$$

Under variable weather conditions, AVC controller needs to recalculate K_{ip} , K_{ii} of G_{ci} , K_{up} , K_{ui} of G_{cu} basing on values of V_{mpp} and I_{mpp} at each new MPP provided by IB technique, so it is also an adaptive controller.

B. SMC controller

1) System of state equations

Write Kirchoff laws in two cases of SW on ($u=1$) and SW off ($u=0$) [22]:

$$\begin{cases} C \frac{dv_{pv}}{dt} = i_{pv} - i_L u \\ R i_L + L \frac{di_L}{dt} = -V_{dc} + v_{pv} u \end{cases} \quad (17)$$

Rewrite system of equations (17), we have system of state equations (18):

$$\begin{cases} \dot{x}_1 = \frac{i_{pv}}{C} - \frac{x_2}{L} u \\ \dot{x}_2 = -\frac{V_{dc}}{L} - \frac{R}{L} i_L + \frac{x_1}{L} u \end{cases} \quad (19)$$

where, $x = [x_1 \ x_2] = [v_{pv} \ i_L]$ is state vector,

$$f(x) = \begin{bmatrix} \frac{i_{pv}}{C} \\ -\frac{V_{dc}}{L} - \frac{R}{L} x_2 \end{bmatrix} \text{ is drift vector field,}$$

$$g(x) = \begin{bmatrix} -\frac{x_2}{C} \\ \frac{x_1}{L} \end{bmatrix} \text{ is control input vector field.}$$

2) Sliding surface

Because of the purpose that reaches to MPP ($m_{ref} = P_{mpp}$) at any time, we choose the following sliding surface (20):

$$S = p_{pv} - P_{mpp} \quad (20)$$

where, P_{mpp} is value of power at MPP (result of IB algorithm) needing to reach at that time (considered as a constant at each time).

3) Stability analysis

According to Lyapunov theory, sliding process will be stable if $S\dot{S} < 0$ [22]. We have:

$$\dot{S} = \frac{d(p_{pv} - P_{mpp})}{dt} \Leftrightarrow \dot{S} = \frac{dv_{pv}}{dt} v_{pv} \left(\frac{i_{pv}}{v_{pv}} + \frac{di_{pv}}{dv_{pv}} \right)$$

so,

$$S\dot{S} = \frac{dv_{pv}}{dt} v_{pv} \left(\frac{i_{pv}}{v_{pv}} + \frac{di_{pv}}{dv_{pv}} \right) (p_{pv} - P_{mpp}) \quad (21)$$

• When the operation is at the left side of MPP and needs to move MPP, we have (22) [4], [13], [17]:

$$\frac{dv_{pv}}{dt} > 0, \frac{i_{pv}}{v_{pv}} + \frac{di_{pv}}{dv_{pv}} > 0, p_{pv} - P_{mpp} < 0 \quad (22)$$

Because of (22), $S\dot{S} < 0$ and the sliding mode process is convergent.

• When the operation is at the right side of MPP and needs to move MPP, we have (23) [4], [13], [17]:

$$\frac{dv_{pv}}{dt} < 0, \frac{i_{pv}}{v_{pv}} + \frac{di_{pv}}{dv_{pv}} < 0, p_{pv} - P_{mpp} < 0 \quad (23)$$

Because of (23), $S\dot{S} < 0$ and the sliding mode process is convergent.

4) Equivalent control signal:

Equivalent control signal $u_{eq}(t)$ is the equivalence between an infinite frequency switched control input (0, 1) and a smooth feedback control. $u_{eq}(t)$ is considered as a smooth feedback control law to maintain ideal state trajectory along S [23]. Value of $u_{eq}(t)$ is determined by (24):

$$0 < u_{eq}(t) = -\frac{L_f S}{L_g S} < 1 \quad (24)$$

where:

$$L_f S = \frac{\partial S}{\partial x^T} f(x) \text{ is deriavation of } S \text{ in the direction of } f(x);$$

$$L_g S = \frac{\partial S}{\partial x^T} g(x) \text{ is deriavation of } S \text{ in the direction of } g(x).$$

Applying for DC/DC buck converter, we have:

$$L_g S = \frac{x_2}{C} \left(i_{pv} + x_1 \frac{\partial i_{pv}}{\partial x_1} \right) \quad (25)$$

$$L_f S = -\frac{i_{pv}}{C} \left(i_{pv} + x_1 \frac{\partial i_{pv}}{\partial x_1} \right) \quad (26)$$

From (25) and (26), $u_{eq}(t)$ is determined by (27):

$$u_{eq}(t) = \frac{i_{pv}}{i_L} \quad (27)$$

5) Control strategy

Control strategy for IB-SMC method is reprinted in Fig. 9.

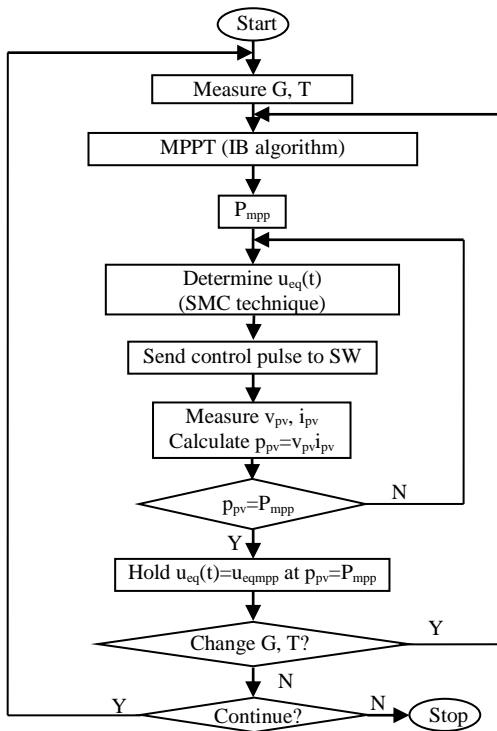


Fig. 9. Control strategy for IB-SMC method

V. SIMULATION

A. Simulation parameters

Parameters of converter, DCbus, and switching frequency are represented in TABLE I. Parameters of PVg type MF165EB3 are represented in TABLE II and n(T) is defined by (28).

TABLE I. PARAMETERS OF CONVERTER, DCbus AND SWITCHING FREQUENCY

	Symbol	Value
DC/DC buck converter	R (Ω)	0.01
	L (H)	5.10 ⁻³
	C (F)	10 ⁻³
Voltage at DCbus	V _{dc} (V)	12
Switching frequency	f _s (kHz)	50

TABLE II. PARAMETERS OF MF165EB3 AT STC

Type of parameters	Symbol	Value
Known parameters provided by manufacturers	I _{SC} (A)	7.36
	V _{OC} (V)	30.4
	V _{mpp} (V)	24.2
	I _{mpp} (A)	6.83
	C _{Ti} (%/°C)	0.057
	C _{Tv} (%/°C)	-0.346
	C _{TP} (%/°C)	-0.478
Unknown parameters calculated by Newton-Raphson algorithm	I _{ph} (A)	7.3616
	I ₀ (A)	1.03.10 ⁻⁷
	V _t (V)	1.6814
	R _s (Ω)	0.2511
	R _p (Ω)	1172.1

$$n(T) = 1 - 0.008017(T - T_{stc}) + \frac{9}{400000}(T - T_{stc})^2 \quad (28)$$

Two offline techniques (CV, Temp) and two online techniques (OV, P&O) using AVC controllers are used to evaluate proposed control methods. Control parameters for above methods are represented in TABLE III.

TABLE III. CONTROL PARAMETERS OF CV-AVC, TEMP-AVC, OV-AVC, P&O

Control method	Control parameters
CV-AVC	V _{mppCV} =24.2 V; K _{ip} = 0.2075; K _{ii} = 4.149; K _{up} = 1.004; K _{ui} = 222.2 (Fixed values)
Temp-AVC (Adaptive controller)	V _{mppTemp} =V _{mppstc} (1+C _{iv} (T-25))
OV-AVC (Adaptive controller)	V _{mppOV} =0.8V _{oc G,T} ; Sample time: 0.4 s Close-circuit time: 0.3 s; Open-circuit time: 0.1 s
P&O	Width pulse control step: Δd=0.2%

Electric energy A(t) each second received from PVg in range time (0÷t) is calculated by (29) and efficiency H% for each control method is calculated by (30):

$$A(t) = \int_0^t p_{pv}(t)dt \quad (29)$$

$$H\% = \frac{A(t)}{A_{mpp}} 100\% \quad (30)$$

B. Simulation results

To see static and dynamic responses and received energy of PVg, a sample scenario for weather condition is considered when T=40°C and the variation of G is represented in Fig. 10.

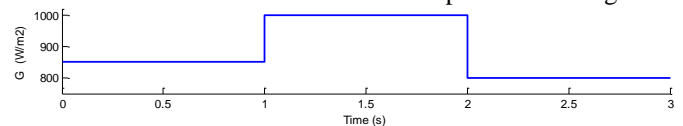


Fig. 10. The variation of G in sample scenario

Fig. 11 presents the process of moving operation points in v-i plane when controller of methods (except OV-AVC method) change control pulse to track MPP in above scenario.

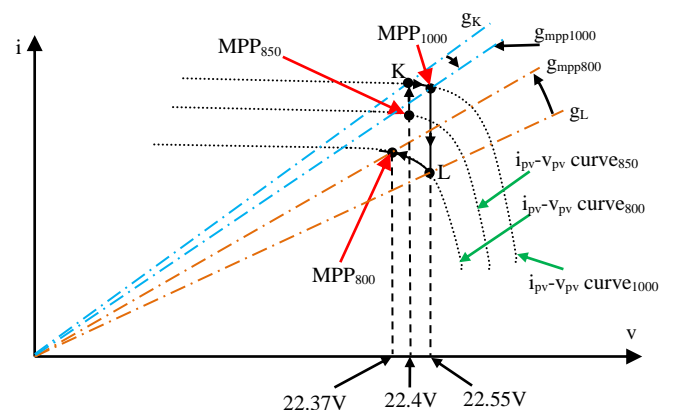


Fig. 11. Process of moving operation points in v-i plane (T=40°C, G varies)

In Fig. 11, starting from MPP_{850} and G increases from 850 W/m^2 to 1000 W/m^2 in Fig. 13, MPP_{850} is moved to K in $v_{pv}-i_{pv}$ curve₁₀₀₀ ($g_{load1}=g_K$) because controllers continue to hold input voltage of the converter at 22.4 V . After MPPT provides new value of voltage at MPP_{1000} (22.55 V), controllers change control pulse to move K to MPP_{1000} (changes g_K to $g_{load2}=g_{mp1000}=0.3$). At the time of decreasing irradiance from 1000 W/m^2 to 800 W/m^2 , MPP_{1000} is immediately moved to L , so controllers continue to change control pulse to hold input voltage of the converter at 22.37 V and move L to MPP_{800} (changes g_L to $g_{load3}=g_{mp800}=0.247$).

Fig. 12 shows $P_{pv}(t)$, P_{mpp} , $A(t)$ for above methods: IB-SMC, IB-AVC, CV-AVC, Temp-AVC, OV-AVC, P&O.

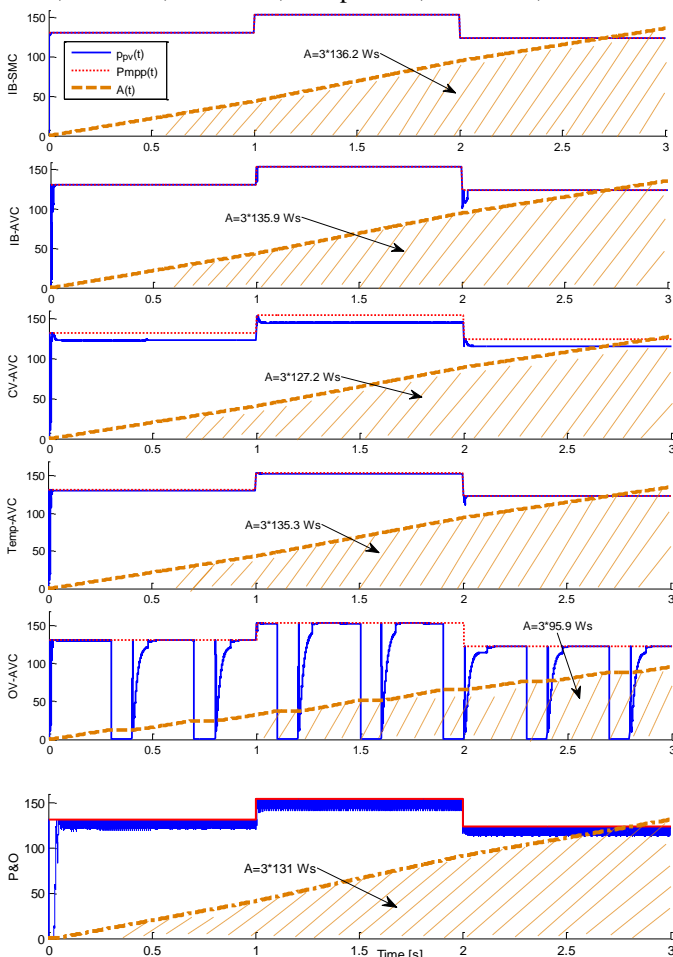


Fig. 12. $p_{pv}(t)$, P_{mpp} , $A(t)$ curves ($T=40^\circ\text{C}$, G varies)

Fig. 13 illustrates efficient curves received by using above methods and corresponding with $G=1000 \text{ W/m}^2$, $G=600 \text{ W/m}^2$ and $G=200 \text{ W/m}^2$ when T increases from 25°C to 65°C . From Fig. 11, Fig. 13, we can see that techniques not using TempS such as OV, CV, P&O always exist some disadvantages: making perturbation in the circuit, causing power loss at the time looking for MPP, operating far MPP and providing medium or low efficiency when weather condition is far STC. If using a TempS, Temp-AVC provides reference value of voltage to the controller quite near voltage at real MPP, flat power curve and track MPP quite well at near STC, so it can use it in some simple application.

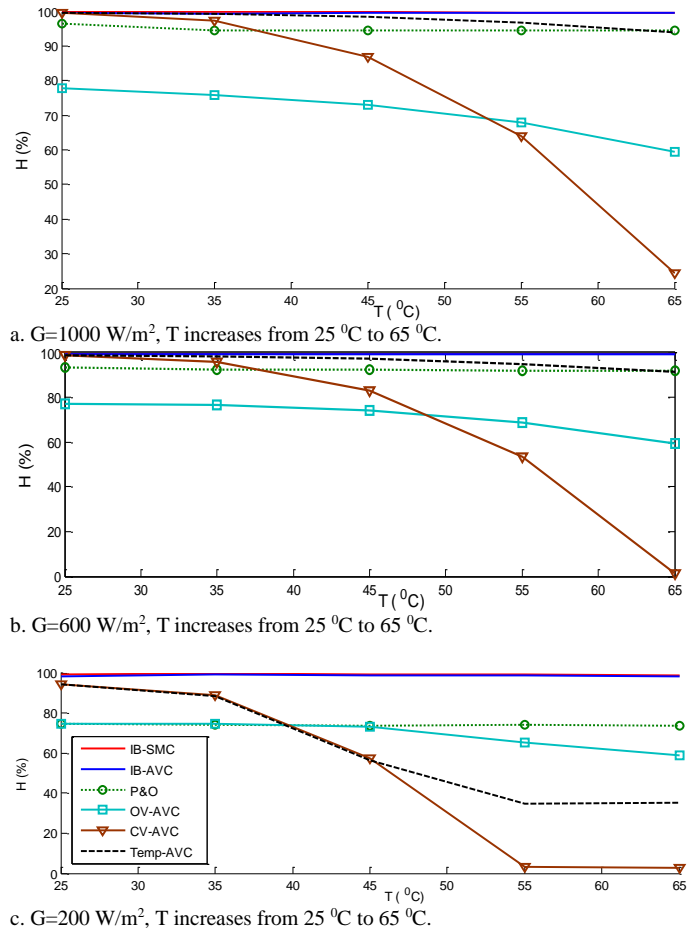


Fig. 13. $A(t)$ curves corresponding with three irradiance levels

IB technique uses both a PYR and a TempS, so it can provide information exactly about MPP at any time. Because of this reason, IB-SMC and IB-AVC methods always have the highest dynamic response to track MPP very well whenever it has any change of weather condition and the highest static response to uphold the operation of PVg at MPP (power curve is always flat) when it doesn't have any change of weather condition. Moreover, these methods also cause very small perturbation and provided the highest efficiency.

IB-SMC and IB-AVC methods also have a significant meaning in combining calculation technique and control techniques through DC/DC converters to help them be easier in real applications with simple microprocessors than traditional techniques. At the same time, they can help us exploit all available energy of PVg at any time to overcome high cost and low efficiency when we use PVg in long time.

VI. CONCLUSION

In this paper, we have presented two new methods to control PVg. They are IB-AVC combining the IB technique with AVC technique and IB-SMC combining IB technique with SMC technique. They use information providing the IB technique, so they use adaptive controllers changing control parameters corresponding with various weather conditions.

Because of using a PYR, TempS, voltage and current sensors, controllers can identify parameters at MPP before creating control pulse, proposed methods overcome disadvantages of previous control methods using online and offline techniques to find MPP. They help controllers improve efficiency (approximately 100%), static and dynamic responses when exploiting PVg.

Simulation results show that the proposed control methods are new approaches to improve the ability to exploit PVg, reduce power loss and perturbation in control circuit and can apply for any structure of PVg. Up to now, PYR and TempS become more popular, it is easier to execute these control methods. IB-SMC method brings higher efficiency a bit than IB-VAC method and provides a dependable tool to test behaviors of PVg in theory. Otherwise, IB-SMC method requires more highly sensitive and accurate measurement units, so IB-VAC method is more suitable and easier to execute in real applications than IB-SMC method.

REFERENCES

- [1] M.G. Villalva, T.G. de Siqueira, E. Ruppert (2010), Voltage regulation of photovoltaic arrays: small-signal analysis and control design, *IET Power Electronic*, Vol. 3, Iss. 6, pp. 869–880.
- [2] Maria C. Mira, Arnold Knott, Ole C. Thomsen, Michael A. E. Andersen (2013), Boost Converter with Combined Control Loop for a Stand-Alone Photovoltaic Battery Charge System, *IEEE 14th Workshop on Control and Modeling for Power Electronics*.
- [3] Hebatallah M. Ibrahim, Jimmy Peng, and Mohamed S. El Moursi (June 2013), Dynamic Analysis of Buck-Based Photovoltaic Array Model, *International Journal of Electrical Energy*, Vol. 1, No. 2.
- [4] Yoash Levron and Doron Shmilovitz (March 2013), Maximum Power Point Tracking Employing Sliding Mode Control, *IEEE Transactions on Circuits and Systems*, Vol. 60, No. 3.
- [5] Omar Boukli-Hacene (September 2013), Robust Regulation of the Photovoltaic Voltage using Sliding Mode Control as Part of a MPPT Algorithm, *International Journal of Computer Applications*, (0975 – 8887), Vol. 78, No.11.
- [6] Ankur V. Rana, Hiren H. Patel (2013), Current Controlled Buck Converter based Photovoltaic Emulator, *Journal of Industrial and Intelligent Information*, Vol. 1, No. 2.
- [7] Emil A. Jimenez Brea, Eduardo I. Ortiz-Rivera (2010), Simple Photovoltaic Solar Cell Dynamic Sliding Mode Controlled Maximum Power Point Tracker for Battery Charging Applications, *Applied Power Electronics Conference and Exposition (APEC), 25th Annual IEEE*.
- [8] Fan Zhang, Jon Maddy, Giuliano Premier, and Alan Guwy (2015), Novel current sensing photovoltaic maximum power point tracking based on sliding mode control strategy, *Solar Energy*, Vol. 118.
- [9] Gaga Ahmed, Errahimi Fatima, ES-Sbai Jania (September 2015), Design and Simulation of a Solar Regulator Based on DC-DC Converters Using a Robust Sliding Mode Controller, *Journal of Energy and Power Engineering*, David Publishing, Vol 9.
- [10] M. Ramesh, S. Sanjeeva Rayudu and R. Polu Raju (2015), A New Approach to Solve Power Balancing Problem in Grid Coupled PV System using Slide Mode Control, *Indian Journal of Science and Technology*, Vol 8(17), August, ISSN (Online): 0974-5645.
- [11] Reham Haroun, Abdelali El Aroudi, Angel Cid-Pastor, Germain Garica, Carlos Olalla, and Luis Martinez-Salamero (June 2015), Impedance Matching in Photovoltaic Systems Using Cascaded Boost Converters and Sliding-Mode Control, *IEEE Transactions on Power Electronics*, Vol. 30, No. 6, June 2015.
- [12] A.B.G. Bahgat, N.H. Helwab, G.E. Ahmadb, E.T. El Shenawy (2005), Maximum Power Point Tracking Controller for PV systems using neural networks, *Renewable Energy*, 30, pp 1257-1268.
- [13] Pawan D. Kale, D.S. Chaudhari (March 2013), A Study of Efficient Maximum Power Point Tracking Controlling Methods for Photovoltaic System, *International Journal of Advanced Research in Computer Science and Software Engineering*, Volume 3, Issue 3.
- [14] Byunggyu Yu (2016), Study on Maximum Power Point Tracking Method Using Open Circuit Voltage, *International Journal of Applied Engineering Research*, ISSN 0973-4562 Volume 11, Number 19.
- [15] Nicola Femia, Member, Giovanni Petrone, Giovanni Spagnuolo, Member, and Massimo Vitelli (July 2005), Optimization of Perturb and Observe Maximum Power Point Tracking Method, *IEEE Transactions on Power Electronics*, Vol. 20, No. 4.
- [16] Mohammed A. Elgendy, Bashar Zahawi, and David J. Atkinson (January 2012), Assessment of Perturb and Observe MPPT Algorithm Implementation Techniques for PV Pumping Applications, *IEEE Transactions on Sustainable Energy*, Vol. 3, No. 1.
- [17] Anmol Ratna Saxena, Shyam Manohar Gupta (2014), Performance Analysis of P&O and Incremental Conductance MPPT Algorithms Under Rapidly Changing Weather Conditions, *Journal of Electrical Systems*, 10-3, 2014.
- [18] Ravinder K. Kharb, Md. Fahim Ansari, S. L. Shimi (January 2014), Design and Implementation of ANFIS based MPPT Scheme with Open Loop Boost Converter for Solar PV Module, *International Journal of Advanced Research in Electrical, Electronics and Instrumentation Engineering*, Vol. 3, Issue 1.
- [19] Roberto F. Coelho, Filipe M. Concer, Denizar C. Martins (2010), A MPPT approach based on temperature measurements applied in PV systems, *IEEE Xplore, International Conference on Industry Applications (INDUSCON)*, 9th IEEE/IAS, Online ISBN: 978-1-4244-8009-8.
- [20] Jiyong Li, Honghua Wang (2009), "Maximum Power Point Tracking of Photovoltaic Generation Based on the Optimal Gradient Method", *Power and Energy Engineering Conference, IEEE*.
- [21] Le Tien Phong, Ngo Duc Minh, Nguyen Van Lien (2015), A New Method to Identify Maximum Power Point for Photovoltaic Generation, *International Conference on Communications, Management and Telecommunications (ComManTel)*, IEEE Xplore, ISBN: 978-1-4673-6546-8.
- [22] Muhammad H. Rashid, "Power electronics handbook", *Academic Press*, International Standard Book Number: 0-12-581650-2, 2001.
- [23] Hebertt Sira-Ramirez, Ramon Silva-Ortigoza, "Control Design Techniques in Power Electronics Devices", *Springer Publisher*, e-ISBN 1-84628-459-7, 2006.



Le Tien Phong, born in 1982, received the M.Sc. degree in 2010 in Electrical Engineering from Ha Noi University of Technology and Science and working in Thai Nguyen University of Technology now. Interested research fields: renewable energy, control electrical energy conversions.



Ngo Duc Minh, born in 1960, received the PhD. degree in Automation from Ha Noi University of Technology and Science in 2010 and working in Thai Nguyen University of Technology now. His research interests include active filter, FACTS BESS, control of power system, distribution grid, renewable energy.



Asc. Prof. Nguyen Van Lien, born in 1949, received the PhD. degree in Power electronic and electric drive in Slovaque university, working in Ha Noi University of Technology and Science now. His research interests include position and motion control, Controlling energy conversion systems in the electric power system and network.